a ~260-bp restriction fragment, and end-labelled. Immunochemical assays were performed as described[28].

Flow cytometry and other assays. Cells were collected with the aid of trypsin and incubated with CM-DCF-DA or NAO (Molecular Probes) at concentrations of 10 and 0.4 μM, respectively, for 20 min at 37C before analysis by flow cytometry[14,15]. To determine the fraction of apoptotic cells after various treatments, cells were stained with the DNA-binding dye H33258 and evaluated by fluorescence microscopy or flow cytometry as described[1]. Superoxide production was assessed with lucigenin[29]. In brief, 4–5 × 10^6 cells were collected with a rubber policeman and resuspended in 1 ml Earle's balanced salt solution (Life Technologies). Dark-adapted lucigenin (bis-*N*-methylacridinium nitrate; Sigma) was added to the samples to 20 μM final concentration. Light emission was detected using a Berthold LB 9505 luminometer for 60 min at 37 °C. Glutathione concentrations were measured using an assay kit (Oxford Biomedical) according to the manufacturer's instructions. Caspase activation was assessed by cleavage of PARP. Lysates from cells infected with Ad-p53 were western-blotted with an anti-PARP antibody and the cleavage fragments quantified by densitometry[4].

Received 27 May; accepted 1 July 1997.

1. Waldman, T., Kinzler, K. W. & Vogelstein, B. p21 is necessary for the p53-mediated G1 arrest in human cancer cells. *Cancer Res.* **55,** 5187–5190 (1995).
2. Oren, M. Relationship of p53 to the control of apoptotic cell death. *Semin. Cancer Biol.* **5,** 221–227 (1994).
3. Velculescu, V. E., Zhang, L., Vogelstein, B. & Kinzler, K. W. Serial analysis of gene expression. *Science* **270,** 484–487 (1995).
4. Polyak, K., Walkman, T., He, T.-C., Kinzler, K. W. & Vogelstein, B. Genetic determinants of p53 induced apoptosis and growth arrest. *Genes Dev.* **10,** 1945–1952 (1966).
5. Levine, A. J. p53, the cellular gatekeeper for growth and division. *Cell* **88,** 323–331 (1997).
6. Lehar, S. M. *et al.* Identification and cloning of Ei24, a gene induced by p53 in etoposide-treated cells. *Oncogene* **12,** 1181–1187 (1996).
7. Hayward, D. C. *et al.* The *sluggish-A* gene of *Drosophila melanogaster* is expressed in the nervous system and encodes proline oxidase, a mitochondrial enzyme involved in glutamate biosynthesis. *Proc. Natl Acad. Sci. USA* **90,** 2979–2983 (1993).
8. Russo, T. *et al.* A p53-independent pathway for activation of WAF1/CIP1 expression following oxidative stress. *J. Biol. Chem.* **270,** 29386–29391 (1995).
9. Reinhoff, H. Y. Jr, Huang, J. H., Li, X. X. & Liao, W. S. Molecular and cellular biology of serum amyloid A. *Mol. Biol. Med.* **7,** 287–298 (1990).
10. Yamaoka, A., Kuwabara, I., Frigeri, I. G. & Liu, F. T. A human lectin, galectin-3 (epsilon bp/Mac-2) stimulates superoxide production by neutrophils. *J. Immunol.* **154,** 3479–3487 (1995).
11. Greenberg, J. T. Programmed cell death: A way of life for plants. *Proc. Natl Acad. Sci. USA* **93,** 12094–12097 (1996).
12. Rao, P. V., Krishna, C. M. & Zigler, J. S. Jr Identification and characterization of the enzymatic activity of zeta-crystallin from guinea *PIG* lens. A novel NADPH : quinone oxidoreductase. *J. Biol. Chem.* **267,** 96–102 (1992).
13. Kroemer, G., Zamzami, N. & Susin, S. A. Mitochondrial control of apoptosis. *Immun. Today* **18,** 45–51 (1997).
14. Zamzami, N. *et al.* Reduction in mitochondrial potential constitutes an early irreversible step of programmed lymphocyte death *in vivo*. *J. Exp. Med.* **181,** 1661–1672 (1995).
15. Petit, P. X. *et al.* Alterations in mitochondrial structure and function are early events of dexamethasone-induced thymocyte apoptosis. *J. Cell. Biol.* **130,** 157–167 (1995).
16. Tamm, I. & Sehgal, P. B. Halobenzimidazole ribosides and RNA synthesis of cells and viruses. *Adv. Virus Res.* **22,** 187–258 (1978).
17. Orrenius, S., Nobel, C. S. I., van den Dobbelsteen, D. J., Burkitt, M. J. & Slater, A. F. G. Dithiocarbamates and the redox regulation of cell death. *Biochem. Soc. Transact.* **24,** 1032–1038 (1996).
18. Holland, P. C., Clark, M. G., Bloxham, D. P. & Lardy, H. A. Mechanism of action of the hypoglycemic agent diphenyleneiodonium. *J. Biol. Chem.* **248,** 6050–6056 (1973).
19. Korsmeyer, S. J. Regulators of cell death. *Trends Genet.* **11,** 101–105 (1995).
20. Susin, S. A. *et al.* Bcl-2 inhibits the mitochondrial release of an apoptogenic protease. *J. Exp. Med.* **184,** 1331–1341 (1996).
21. Yang, J. *et al.* Prevention of apoptosis by Bcl-2: release of cytochrome *c* from mitochondria blocked. *Science* **275,** 1129–1132 (1997).
22. Kluck, R. M., Bossy-Wetzel, E., Green, D. R. & Newmeyer, D. D. The release of cytochrome *c* from mitochondria: a primary site for Bcl-2 regulation of apoptosis. *Science* **275,** 1132–1136 (1997).
23. Borek, C. Radiation and chemically induced transformation: free radicals, antioxidants and cancer. *Br. J. Cancer suppl.* **8,** 74–86 (1987).
24. Vayssiere, J. L., Petit, P. X., Risler, Y. & Mignotte, B. Commitment to apoptosis is associated with changes in mitochondrial biogenesis and activity in cell lines conditionally immortalized with simian virus 40. *Proc. Natl Acad. Sci. USA* **91,** 11752–11756 (1994).
25. Johnson, T. M., Yu, Z.-X., Ferrans, V. J., Lowenstein, R. A. & Finkel, T. Reactive oxygen species are downstream mediators of p53-dependent apoptosis. *Proc. Natl Acad. Sci. USA* **93,** 11848–11852 (1996).
26. El-Diery, W. S. *et al.* WAF1, a potential mediator of p53 tumor suppression. *Cell* **75,** 817–825 (1993).
27. Velculescu, V. E. *et al.* Characterization of the yeast transcriptome. *Cell* **88,** 243–251 (1997).
28. El-Deiry, W. S., Kern, S. E., Pietenpol, J. A., Kinzler, K. W. & Vogelstein, B. Definition of a consensus binding site for p53. *Nature Genet.* **1,** 45–49 (1992).
29. Faulkner, K. & Fridovich, I. Luminol and lucigenin as detectors for O_2^-. *Free Rad. Biol. Med.* **15,** 447–451 (1993).

Acknowledgements. We thank V. Velculescu, L. Zhang and W. Zhou for help with SAGE analysis; J. A. Duine for bongkrekic acid; J. Flook for assistance with flow cytometry; and members of our laboratories for discussion. This work was supported by the Clayton Fund and by grants from the NIH. K.P. is a research associate and B.V. is an investigator of the Howard Hughes Medical Institute.

Correspondence and requests for materials should be addressed to K.W.K.

Self-organization of microtubules and motors

F. J. Nédélec*†, T. Surrey*, A. C. Maggs† & S. Leibler*

** Departments of Molecular Biology and Physics, Princeton Unviersity, Princeton, New Jersey 08544, USA*
Laboratoire de Physico-Chimie Théorique, Ecole Supérieure de Physique et Chimie Industrielles, 10 rue Vauquelin, 75231 Paris, France

Cellular structures are established and maintained through a dynamic interplay between assembly and regulatory processes. Self-organization of molecular components provides a variety of possible spatial structures: the regulatory machinery chooses the most appropriate to express a given cellular function[1]. Here we study the extent and the characteristics of self-organization using microtubules and molecular motors[2] as a model system. These components are known to participate in the formation of many cellular structures, such as the dynamic asters found in mitotic and meiotic spindles[3,4]. Purified motors and microtubules have previously been observed to form asters *in vitro*[5]. We have reproduced this result with a simple system consisting solely of multi-headed constructs of the motor protein kinesin[6] and stabilized microtubules. We show that dynamic asters can also be obtained from a homogeneous solution of tubulin and motors. By varying the relative concentrations of the components, we obtain a variety of self-organized structures. Further, by studying this process in a constrained geometry of micro-fabricated glass chambers[7], we demonstrate that the same final structure can be reached through different assembly 'pathways'.

A dividing cell has to separate spatially its newly duplicated chromosomes. It uses the bipolar spindle, a complex molecular structure made of many different protein components, to accomplish this task with high precision. Spindle formation is an intensively studied prototype of cell morphogenesis phenomena. A bipolar spindle forms when mitotic chromosomes capture and selectively stabilize dynamic microtubules nucleated by two centrosomes[1]. This assembly process tolerates numerous variations in intermediate configurations, such as different chromosome positions and geometrical and mechanical perturbations[8]. Spindles

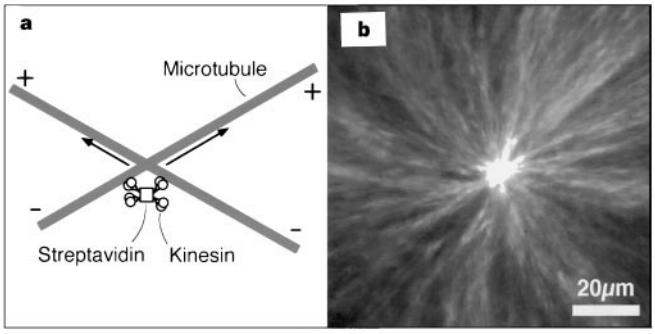

Figure 1 Self-organization of taxol-stabilized microtubules and kinesin constructs into asters. **a**, Schematic representation of a kinesin–streptavidin construct moving simultaneously along two microtubules. The kinesin constructs can be seen as force-generating, mobile crosslinks. **b**, A self-organized aster observed by dark-field microscopy. Polymerized and taxol-stabilized microtubules were mixed with motor constructs and ATP. The sample is shown after ~2 min. The bright spot in the centre of the aster is caused by light scattering from accumulated microtubules and motors. In cells and cell-free extracts, where the asters are organized by minus-end directed motors such as dyneins[16,17], the aster polarity is opposite. Scale bar, 20 μm.

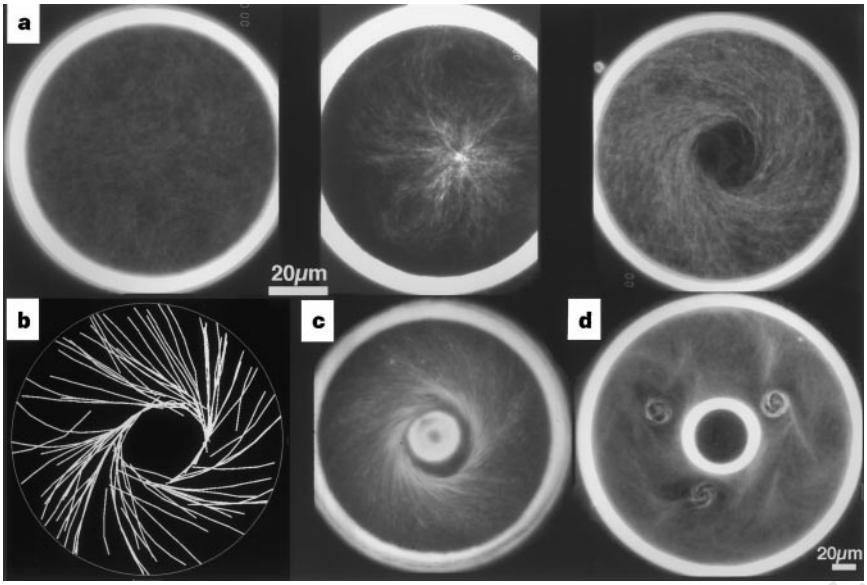

Figure 2 Self-organization in the constrained geometry of micro-fabricated chambers etched in glass. **a**, Formation of a vortex as observed by dark-field microscopy in a chamber of diameter 90 μm and depth 5 μm. Microtubule polymerization has been initiated by warming to 37 °C. Left, after ~0.5 min, microtubules nucleate uniformly in the sample; middle, after ~1.5 min, an aster forms in the centre of the chamber; right, after ~3 min, a steady-state vortex structure is observed. **b**, Two-dimensional numerical simulation of the same process. The microtubule mean length was initially smaller than the chamber radius, but became longer than it in the state shown. **c**, Vortex structure in a torus-shaped chamber of the same diameter as previously, but including a central unetched region. **d**, Steady-state structure in a torus-shaped chamber of larger size (240 μm). The three vortices have the same core size as those in **a** and **c**. Scale bars, 20 μm.

also form in the absence of centrosomes, as observed in meiotic cell divisions, and, more surprisingly, in *in vitro* experiments in *Xenopus laevis* egg extracts devoid of centrosomes[9,10], in which case microtubules grown in the vicinity of chromatin are organized into bipolar spindle by molecular motors.

In order to explore the issues of self-organization of mitrotubules and motors, we have constructed an extremely simplified system with only a few purified components. In addition to tubulin, this system includes artificial molecular constructs of several kinesin heads associated through biotin–streptavidin links. We chose kinesin because of its extensive molecular characterization[11–13]. The motor constructs (kinesins or motors) attach to neighbouring microtubules and, in the presence of ATP, move towards the microtubule 'plus' ends[14]. In this way they form dynamic crosslinks between microtubules (Fig. 1a).

An aster formed in a system of microtubules stabilized with taxol[15] and mixed with motors is shown in Fig. 1b. The sample is sandwiched between slide and coverslip in a quasi-two-dimensional geometry. The starting configuration is an isotropic 'gel' consisting of microtubules crosslinked randomly by motors (not shown). Asters of microtubules form within a few minutes as kinesins accumulate in their centres. The size of the asters is expected to be determined by the length distribution of stabilized microtubules. Similar asters were previously observed to form in a system of purified heavy chains of kinesin mixed with microtubules[5], as well as in *Xenopus laevis* egg extracts with the addition of microtubule stabilizing agents[16,17].

The use of taxol allows us to control microtubule length and number, although stabilizing microtubules with taxol is not necessary for aster formation: asters also form if microtubules are allowed to assemble and disassemble through the dynamic instability[18]. All further experiments, presented below, are performed in the absence of taxol.

To study the influence of geometrical constraints on self-organization, we have encapsulated solutions of tubulin and motors in sealed micro-fabricated glass chambers[7] of various shapes, with typical lateral dimensions of 100 μm and a thickness of 5 μm (Fig. 2). In a cylindrical geometry, microtubules polymerizing from an initially homogeneous solution first organize into a symmetric aster centred in the chamber. As microtubules continue to grow and begin to buckle, the centre of the aster becomes unstable and a vortex structure forms. Vortices can be observed simultaneously in hundreds of chambers etched in a single coverslip and filled with the same initial solution. We saw an equal number of structures with right-handed and left-handed vorticity. Because vortices form from asters, the microtubules have their plus ends oriented towards the centre of the vortex. Small objects, such as short microtubules or small colloidal beads with motors attached to them, circle around the core of the vortex. This circulatory motion is reminiscent of the microtubule- and motor-dependent movement of cytoplasm observed in the development of *Drosophila melanogaster* oocytes[19].

One advantage of using highly simplified systems with a small number of well-characterized components is the accessibility to quantitative theoretical analysis. Aster formation can be studied in numerical simulations, in which microtubules are treated as flexible, polar rods, and kinesin-like motors are characterized by a linear force–velocity curve[11,12] and high processivity[11,12]. Vortices can also be reproduced in numerical simulation by incorporating geometrical confinement and the dynamic assembly of microtubules (Fig. 2b). This simulation exhibits an assembly pathway very similar to that in the experiments, in which an initially symmetric aster is destabilized by the growth and buckling of microtubules.

To determine whether assembly through a symmetric aster is the only possible route leading to the final vortex structure, we enclosed the same solution of proteins in a chamber of the same size but with the topology of a torus. The idea for this came from experiments of microsurgery performed on melanophores[20] in which the geometry of the cell was changed artificially. The formation of symmetric asters is now prevented by the geometry of the chamber, but the same final steady state, a vortex, can nevertheless be reached (Fig. 2c), demonstrating that this simple system can find alternative 'assembly pathways'. This is similar to results obtained in *Xenopus laevis* egg extracts, in which microtubule asters were formed either around centrosomes or through motor-mediated assembly[9,10]. The existence of alternative 'assembly pathways' can be of more general importance. It is easy to imagine that, as in the case of metabolic or signal transduction pathways, a given route of assembly could be selected depending on cell type, interactions with the environment, or state of growth.

Further experiments have shown that the precise shape of the containers is often unimportant for the choice of final assembled structures. For instance, we have regularly observed formation of circular vortices in square chambers (data not shown). However, in a chamber of the same torus-like shape but of a larger lateral size, a different final structure is observed (Fig. 2d).

A surprising variety of larger-scale patterns can be formed in an unconfined geometry by further self-organization of the previously

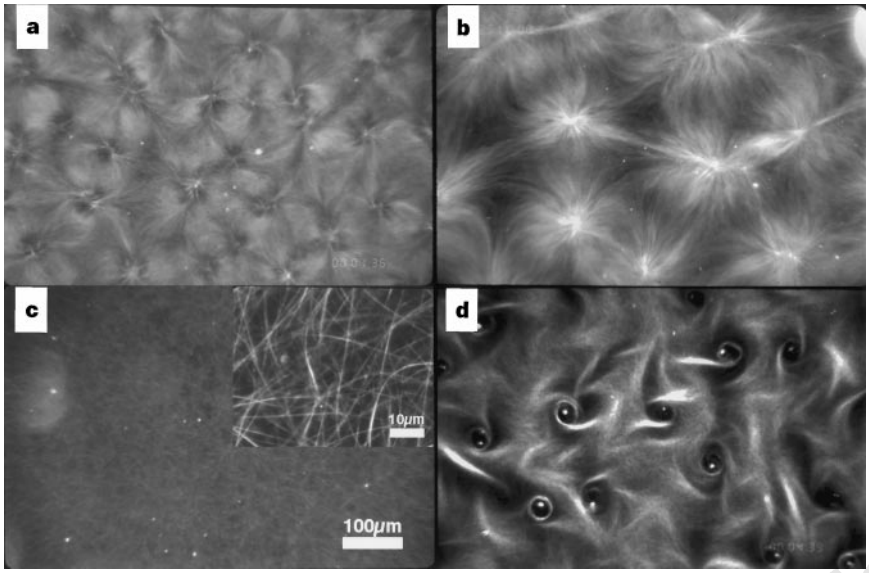

Figure 3 Different large-scale patterns formed through self-organization of microtubules and motors. Initially uniform mixtures of proteins were heated to 37 °C, and patterns resulting after 7 min are shown at equal magnification. The samples differ in kinesin concentration. **a**, A lattice of asters and vortices obtained at ~25 μg ml^{-1} kinesin. **b**, An irregular lattice of asters obtained at ~37.5 μg ml^{-1} kinesin. **c**, Microtubules form bundles at ~50 μg ml^{-1} kinesin (scale bar, 100 μm). Insert, at higher magnification (scale bar, 10 μm). **d**, A lattice of vortices obtained at <15 μg ml^{-1} kinesin.

described structural elements, asters and vortices. The final patterns depend on the initial concentrations of molecular components: a twofold variation in the concentration of kinesin, included in the same solution of assembling microtubules, results in quite different patterns (Fig. 3). At low motor concentrations a lattice of vortices forms, but at slightly higher kinesin concentrations lattices of asters can be observed. Although the asters obtained in our simplified systems are similar to those observed in cells or cellular extracts, the precise dynamical parameters characterizing both microtubules and motors are very different. When two neighbouring asters overlap sufficiently, they can merge, and this process may determine the final distance between the asters. Finally, at even higher motor concentrations, a distinct state is achieved in which the microtubules form bundles. This process is sensitive to the microtubule nucleation rate, and depends on the ionic conditions.

We have shown that the dynamics of microtubules and motors has to be controlled for a desired structure, such as an aster or a vortex, to be obtained. In our simplified systems this is achieved by controlling the motor and tubulin concentrations. However, in the cellular context the choice of different structures does not necessarily involve the precise variation of relative protein concentrations, but rather the control of their activities. The cell can control the action of motors and the dynamics of microtubule assembly through various regulatory processes, such as covalent modifications and binding of associated proteins[21,22].

The self-organization we have observed can be compared to the pattern formation encountered in simple physical systems[23], in which a variety of structures has been formed far from thermal equilibrium from a homogeneous solution of proteins and from a gel of fibres, connected through non-covalent dynamic crosslinks. The energy dissipated in these structures is injected into the system through ATP and GTP hydrolysis[24]. From this point of view, the situation is reminiscent of patterns formed in chemical reactions[23]. The use of protein components, however, means that there is the possibility of additional control at the molecular level. A complete characterization of the phenomena described here should really include an evaluation of all the relevant time and length scales, and the determination of the out-of-equilibrium phase diagrams.

These simplified experiments show that the basic structural 'vocabulary' used by the cell is extremely rich. By using just two basic components and simple local rules of interaction, we obtained a large variety of assembled structures. By extending our system as to include other interacting components, such as nucleation centres for microtubules or different motors, it will be possible to explore the conditions and the components needed for the formation other structures. Another direction of study would be to introduce some elements of regulation, making it possible to search for rules underlying the choice of different 'words' from this large 'vocabulary' of self-organized structures. □

Methods

Proteins. Recombinant kinesin K401-bio, consisting of 401 amino acids of the N-terminal motor domain of the heavy chain of *D. melanogaster* kinesin linked to the BCCP sequence of *Escherichia coli*, was expressed in *E. coli* and purified[25]. These recombinant kinesins form biotinylated active dimers[25], which can then be joined by adding streptavidin[26] (Molecular Probes). A solution of motor constructs was obtained by mixing streptavidin and purified K401-bio, giving final concentrations of 30 μg ml^{-1} and ~150 μg ml^{-1}, respectively. Complex formation was verified by gel filtration and light scattering. Tubulin was purified from bovine brain[6]; the stock solution was at ~15.3 mg ml^{-1} in storage buffer (80 mM PIPES and KOH to pH 6.8, 2 mM $MgCl_2$, 1 mM EGTA).

Assay with stabilized microtubules. To polymerize microtubules, a solution containing 1.25 mg ml^{-1} tubulin, 1 mM GTP, 1% DMSP in storage buffer was kept at 37 °C for 15 min, and taxol was then added to a final concentration of 20 μM. Polymerized microtubules were kept at room temperature. To start self-assembly, polymerized microtubules, motor constructs and ATP solution were mixed to give final concentrations of 0.27 mg ml^{-1} tubulin, 50 μg ml^{-1} K401-bio, 10 μg ml^{-1} Streptavidin, 1.4 mM ATP, 0.6 mM GTP, 7.7 mM $MgCl_2$, 4.3 mM KCl, 1 mM EGTA, 27 μg ml^{-1} α-casein (Sigma), 0.3% DMSO, 20 μm taxol, 80 mM PIPES/KOH to pH 6.8. This mixture was immediately examined by microscopy. Kinesin K401-bio moves microtubules with typical speeds up to ~0.8 μm s^{-1} in motility assays (data not shown). We have varied the relative amount of streptavidin to kinesin and found that the maximum activity in motility assays is observed at a stochiometric ratio of approximately four K401-bio dimers per streptavidin tetramer; this ratio was used for all experiments. The precise ratio of active kinesins per streptavidin might vary to some extent in our experiments owing to some variability of the kinesin activity of different purifications. All experiments were performed several times and the resulting structures were found to be reproducible. No asters are formed without streptavidin or with too much streptavidin. In the absence of ATP, a crosslinked gel of microtubules forms not showing any further temporal evolution.

Assay with non-stabilized, dynamic microtubules. A mixture of purified (unpolymerized) tubulin, motor constructs and nucleotides was now used. Apart from an increased tubulin concentration of 5.1 mg ml^{-1} and absence of taxol, all other concentrations were kept as in the assay with stabilized microtubules, unless specified otherwise. Polymerization of microtubules was started by heating the sample to 37 °C on the microscope.

Glass cleaning and coating. VWR-brand 24 × 60 mm no. 1 coverslips were cleaned by three rounds of sonication in a hot solution (~80 °C) of 10% detergent VWR-Extran 1000 in de-ionized water, followed by 5 rounds of

sonication in pure, hot, de-ionized water. Slides were then immersed in pure ethanol and air-dried. Glass cleaned this way was hydrophilic. To prevent kinesin and microtubules from sticking to the surface, slides were coated by dipping them into a solution of 0.1% agarose in de-ionized water and were allowed to dry. This layer was further coated by dipping the glass first into a solution of 0.2% bovine serum albumin in storage buffer filtered at 0.2 μm, and then four times into de-ionized water. Coated slides were kept humid and were used within a few hours.

Fabrication of microchambers. This was performed as described previously[6]. Glass with microfabricated chambers was cleaned and coated as usual. Sealing of the microchambers was achieved by applying a steady ~20 kg cm^{-2} pressure for 3 min on the pit-containing coverslip and the slide.

Microscopy and imaging. A Zeiss Axiovert 135 TV with an Olympus 100× iris objective, an Olympus 20× objective and a Zeiss dark-field ultra condenser was used. Both condenser and objective were heated to warm the immersion oil and the sample to 37 °C by circulating warm water through copper tubing wrapped around them. A CCD camera (Paultek) was used to record on S-VHS video tape, and no video processing was necessary to observe microtubules. A Nikon camera was also mounted on the microscope to take slides with Kodak Ektachrome P1600 film.

Simulations. Simulations will be described in detail elsewhere (F.N. *et al.*, manuscript in preparation). Briefly, microtubules were represented by short rigid rods of 6 μm connected with flexible links: they could grow and shrink according to a simple model of dynamic instability[27]. The simulations were two-dimensional; this corresponds well to experiments performed in thin chambers or between closely spaced glass surfaces, in which microtubules are nearly parallel to the plane of the sample. Motor complexes could bind up to two microtubules. Unbound complexes could diffuse freely, whereas complexes bound to two microtubules exerted a spring-like force between them. The movement of the microtubules was then calculated at each time step by assuming a completely damped viscous regime. At each time step, motors moved along the microtubules with a speed that is a function of the force they exert. Relevant parameters are known from previous experiments, such as a polymerization speed of 2 μm min^{-1} (ref. 28), a microtubule persistence length of 5 mm (ref. 29), a linear force–speed curve with maximum speed 0.8 μm s^{-1}, and a maximum force of 5 pN (refs 10, 11). A typical simulation covered 10 min of real time.

Received 19 March; accepted 13 June 1997.

1. Kirschner, M. & Mitchison, T. Beyond self-assembly: From microtubules to morphogenesis. *Cell* **45,** 329–342 (1986).
2. Howard, J. The movement of kinesin along microtubules. *Annu. Rev. Physiol.* **58,** 703–729 (1996).
3. Hyman, A. & Karsenti, E. Morphogenetic properties of microtubules and mitotic spindle assembly. *Cell* **84,** 401–410 (1996).
4. Barton, N. R. & Goldstein, L. S. B. Going mobile: Microtubule motors and chromosome segregation. *Proc. Natl Acad. Sci. USA* **93,** 1735–1742 (1996).
5. Urrutia, R., McNiven, M., Albanesi, J., Murphy, D. & Kachar, B. Purified kinesin promotes vesicle motility and induces active sliding between microtubules in vitro. *Proc. Natl Acad. Sci. USA* **88,** 6701–6705 (1991).
6. Berliner, E. *et al.* Microtubule movement by a biotinilated kinesin bound to a streptavidin-coated surface. *J. Biol. Chem.* **269,** 8610–8615 (1994).
7. Holy, T., Dogterom, M., Yurke, B. & Leibler, S. Assembly and positioning of microtubule asters in microfabricated chambers. *Proc. Natl Acad. Sci. USA* **94,** 6228–6233 (1997).
8. Nicklas, R. B. & Ward, S. C. Elements of error correction in mitosis: microtubule capture, release, and tension. *J. Cell Biol.* **126,** 1241–1253 (1994).
9. Heald, R. *et al.* Self-organization of microtubules into bipolar spindles around artificial chromosomes in *Xenopus* egg extracts. *Nature* **382,** 420–425 (1996).
10. Sawin, K. E. & Mitchison, T. Mitotic spindle assembly by two different pathways in vitro. *J. Cell Biol.* **112,** 925–940 (1991).
11. Hunt, A. J., Gittes, F. & Howard, J. The force exerted by a single molecule against a viscous load. *Biophys. J.* **67,** 766–781 (1994).
12. Svoboda, K. & Block, S. M. Force and velocity measured for single kinesin molecules. *Cell* **77,** 773–784 (1994).
13. Mayhofer, E. & Howard, J. The force generated by a single kinesin molecule against an elastic load. *Proc. Natl Acad. Sci. USA* **92,** 574–578 (1995).
14. Kashina, A. S. *et al.* A bipolar kinesin. *Nature* **379,** 270–272 (1996).
15. Arnal, I. & Wade, R. How does taxol stabilize microtubules? *Curr. Biol.* **5,** 900–908 (1995).
16. Verde, F., Berrez, J.-M., Antony, C. & Karsenti, E. Taxol-induced microtubule asters in mitotic extracts of *Xenopus* eggs: Requirement for phosphorylated factors and cytoplasmic dynein. *J. Cell Biol.* **112,** 1177–1187 (1991).
17. Stearns, T. & Kirschner, M. In vitro reconstitution of centrosome assembly and function: The central role of gamma-tubulin. *Cell* **76,** 623–637 (1994).
18. Mitchison, T. & Kirschner, M. Microtubule assembly nucleated by isolated centrosomes and dynamic instability of microtubule growth. *Nature* **312,** 232–242 (1984).
19. Theurkauf, W. E. Premature microtubule-dependent cytoplasmic streaming in cappucino and spire mutant oocytes. *Science* **265,** 2093–2096 (1994).
20. Rodionov, V. & Borisy, G. G. Self-centring activity of cytoplasm. *Nature* **386,** 170–173 (1997).
21. Vernos, I. & Karsenti, E. Motors involved in spindle assembly and chromosome segregation. *Curr. Opin. Cell Biol.* **8,** 4–9 (1996).
22. McNally, F. J. Modulation of microtubule dynamics during the cell cycle. *Curr. Opin. Cell Biol.* **8,** 23–29 (1996).
23. Cross, M. C. & Hohenberg, P. C. Pattern formation outside of equilibrium. *Rev. Mod. Phys.* **65(2)** (1993).
24. Tabony, J. Morphological bifurcations involving reaction–diffusion processes during microtubule formation. *Science* **264,** 245–248 (1994).
25. Young, E. C., Berliner, E., Mahtani, H., Perez-Ramirez, B. & Gelles, J. Subunit interactions in dimeric kinesin heavy chain derivatives that lack the kinesin rod. *J. Biol. Chem.* **270,** 3926–3931 (1995).
26. Bayer, E. & Wilchek, M. Avidin and streptavidin. *Methods Enzymol.* **184,** 51–67 (1990).
27. Dogterom, M., Leibler, S. Physical aspects of the growth and regulation of microtubule structures. *Phys. Rev. Lett.* **20,** 1347–1350 (1993).
28. Erickson, H. & O'Brien, E. Microtubule dynamic instability and GTP hydrolysis. *Annu. Rev. Biophys. Biomol. Struct.* **21,** 145–166 (1992).
29. Gittes, F., Mickey, B., Nettleton, J. & Howard, J. Flexural rigidity of microtubules and actin filaments measured from thermal fluctuations in shape. *J. Cell Biol.* **120,** 923–934 (1993).

Acknowledgements. We thank E. Young and J. Gelles for kinesin plasmids; J. Johnson for taxol; T. Holy for help with the preparation of glass chambers; and T. Holy, M. Elowitz, E. Wolf, E. Karsenti, T. Mitchison, J. Howard and S. Block for discussions. This work was supported by grants from the NIH, the NSF and the HFSP, a fellowship from the Deutsche Forschungsgemeinschaft (T.S.) and the French Government (F.J.N.).

Correspondence and requests for materials should be addressed to S.L. (e-mail: leibler@princeton.edu).

Structure of a viral procapsid with molecular scaffolding

Terje Dokland*, Robert McKenna*†, Leodevico L. Ilag*†, Brian R. Bowman*†, Nino L. Incardona‡, Bentley A. Fane§ & Michael G. Rossmann*

* *Department of Biological Sciences, Purdue University, West Lafayette, Indiana 47907-1392, USA*

‡ *Department of Microbiology and Immunology, University of Tennessee, Memphis, Tennessee 38163, USA*

§ *Department of Biological Sciences, University of Arkansas, Fayetteville, Arkansas 72701, USA*

The assembly of a macromolecular structure proceeds along an ordered morphogenetic pathway, and is accomplished by the switching of proteins between discrete conformations as they are added to the nascent assembly[1–3]. Scaffolding proteins often play a catalytic role in the assembly process[1,2,4], rather like molecular chaperones[5]. Although macromolecular assembly processes are fundamental to all biological systems, they have been characterized most thoroughly in viral systems, such as the icosahedral *Escherichia coli* bacteriophage ΦX174 (refs 6, 7). The ϕX174 virion contains the proteins F, G, H and J[7,8]. During assembly, two scaffolding proteins B and D are required for the formation of a 108S, 360-Å-diameter procapsid from pentameric precursors containing the F, G and H proteins[6,9]. The procapsid contains 240 copies of protein D, forming an external scaffold, and 60 copies each of the internal scaffolding protein B, the capsid protein F, and the spike protein G[9,10]. Maturation involves packaging of DNA and J proteins and loss of protein B, producing a 132S intermediate[6,7]. Subsequent removal of the external scaffold yields the mature virion. Both the F and G proteins have the eight-stranded antiparallel β-sandwich motif[8,11] common to many plant and animal viruses[12,13]. Here we describe the structure of a procapsid-like particle at 3.5-Å resolution, showing how the scaffolding proteins coordinate assembly of the virus by interactions with the F and G proteins, and showing that the F protein undergoes conformational changes during capsid maturation.

For the structure determination we obtained a low-resolution, 6.5-Å data set collected from a single, frozen crystal, and a higher-resolution, 3.5-Å data set collected from a number of crystals at 4 °C (Table 1). The structure was solved to nearly 3.5-Å resolution by molecular-replacement real-space averaging[14], using a starting model based on the previously determined electron-microscopic

† Present addresses: Department of Biological Sciences, Warwick University, Coventry CV4 7AL, UK (R.M.); Morphosys GmbH, Frankfurter Ring 193a, 80807 München, Germany (L.L.I.); Department of Biochemistry, Baylor College of Medicine, Houston, Texas 77030, USA (B.R.B.).